Acta Cryst. (1994). B50, 649–655

The Low-Temperature Structure of $NbTe_4$

BY J. KUSZ* AND H. BÖHM

Institut für Geowissenschaften der Universität, D-55099 Mainz, Germany

(*Received* 13 *January* 1994; *accepted* 12 *May* 1994)

Abstract

The incommensurate room-temperature (RT) structure of $NbTe_4$ undergoes a phase transition into an intermediate incommensurate low-temperature (LT) phase at low temperatures, before the lock-in transition into the commensurate low-temperature (C) phase occurs at *ca* 50 K. In an X-ray experiment, the additional satellite reflections of the intermediate low-temperature phase are diffuse at room temperature, but remain diffuse in one dimension (along c^*) also at very low temperatures. A structure determination has been carried out for the LT phase with the diffuse satellite reflections based on a data set which was measured at 100 K. The incommensurate LT structure is described as a $(2 \times 2 \times 3)$-fold superstructure approximation. In a supercell, the formation of triplets of Nb atoms with phase shifts of $2/3\pi$ between neighbouring chains are found. The final R value in the space group $P4$ is $R = 0.060$.

1. Introduction

Transition-metal tetrachalcogenides such as $NbTe_4$ are compounds exhibiting a pseudo-one-dimensional character in the structure. The basic structure has been determined by Selte & Kjekshus (1964). The Te atoms form one-dimensional infinite columns of stacked tetragonal antiprisms along [001], which are centred by the Nb atoms [$P4/mcc$, Fig. 1(*a*)]. In Fig. 1(*b*), projections of such columns along the c-axis are depicted as a scheme of Te squares. In the basic structure of Selte & Kjekshus (1964), the columns denoted by A, B, C and D are identical. As for other transition-metal chalcogenides of this type, distortions attributed to charge-density waves have been observed by Boswell, Prodan & Brandon (1983) and Böhm & von Schnering (1983). These authors have shown that at room temperature, the modulation is incommensurate with the wave vector $\mathbf{q}_1 = (1/2,1/2, 0.688)$. A first structure determination by Böhm & von Schnering (1983) was based on a threefold superstructure; it showed the characteristic deformation modes of the basic structure: Nb is longitudinally modulated along the c-axis; for Te, both a longitudinal mode and a transversal breathing mode and a libration of the Te-squares were determined. A structure determination by van Smaalen, Bronsema & Mahy (1986), based on the superspace group $W^{P4/mcc}_{1\,111}$, is consistent with the distortion modes found by Böhm & von Schnering (1985) for a threefold superstructure (Kusz & Böhm, 1992).

The diffraction patterns of $NbTe_4$ are characterized by three classes of reflections, as shown in the schematic diagram of Fig. 2:

(i) by main reflections, they are related to the average structure, which corresponds to the basic structure;
(ii) by one class of satellite reflections, they can be observed up to the fourth order by X-rays; the **q**-vector is $\mathbf{q}_1 = (1/2,1/2,q_z)$;
(iii) by another class of satellite reflections, for $NbTe_4$ they are diffuse at room temperature; these reflections are described by the **q**-vectors $\mathbf{q}_2 = (1/2,0,q_z)$, $\mathbf{q}_3 = (0,1/2,q_z)$.

The **q**-vector notation is based on the cell of the basic structure. The indexing of reflections in the reciprocal lattice, however, is for convenience based on a $(2 \times 2 \times 3)$-fold superstructure, $2a_0 \times 2b_0 \times 3c_0$, in the incommensurate case as well.

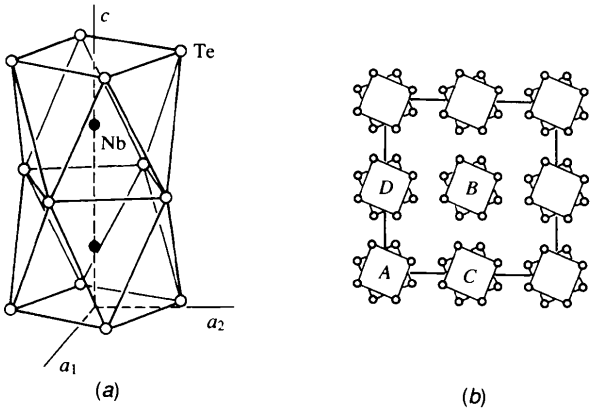

Fig. 1. (*a*) The basic structure of $NbTe_4$; (*b*) Te squares are depicted as a projection on the (a_1,a_2) plane.

* On leave from the Institute of Physics, University of Silesia, Katowice, Poland.

Most incommensurately modulated phases transform into a commensurate low-temperature phase on cooling (lock-in transition). Such a phase transition has also been observed for $NbTe_4$ in the electron diffraction pattern by Eaglesham, Bird, Withers & Steeds (1985) and Mahy, van Landuyt, Amelinckx, Bronsema & van Smaalen (1986). The transformation apparently occurs in two steps. On cooling from room temperature, pairs of the additional ($\mathbf{q}_2$,$\mathbf{q}_3$)-satellites appear at an intermediate position between two pairs of incommensurate $\mathbf{q}_1$-satellites in the (a_1*,c*)-plane (Fig. 2). These ($\mathbf{q}_2$,$\mathbf{q}_3$)-satellites can be anticipated even at room temperature as diffuse spots in the X-ray diffraction pattern. They become sharp (at *ca* 140–120 K) in two dimensions within the (a_1*,a_2*)-plane (first step), but they remain diffuse until they also become sharp in the third dimension at *ca* 50 K (second step). The new satellites as well as the $\mathbf{q}_1$–satellites are then at commensurate positions of a threefold superstructure (lock-in transition). Boswell & Prodan (1986) report that in the electron diffraction pattern the diffuse ($\mathbf{q}_2$,$\mathbf{q}_3$)-satellites develop into closely spaced sharp satellites before the lock-in transition at *ca* 50 K. As reported by Kusz & Böhm (1993), the second step of the phase transition does not occur in an X-ray experiment with a macroscopic crystal. On cooling, the diffuse ($\mathbf{q}_2$,$\mathbf{q}_3$)-satellites also become sharp in two dimensions, however, even at 10 K they remain diffuse in the c*-direction with a peak intensity at the commensurate value of $q_z = 2/3$.

2. Low-temperature experiments

Needle-shaped single crystals of $NbTe_4$ were synthesized from the elements in a procedure similar to that reported by Selte & Kjekshus (1964). The size of the crystal used was 0.1 × 0.1 × 0.8 mm, with the longest edge being the c-axis.

The reflections were measured on a four-circle κ-diffractometer (Enraf–Nonius CAD-4) with a graphite monochromator [Mo $K\alpha$ radiation (0.7107 Å)] and a liquid nitrogen cooling device. The intensities of the sharp satellites were measured at the commensurate positions of c*/3 up to second order; the higher-order satellites were too weak to be observed. When cooling from room temperature, the data set changed, additional ($\mathbf{q}_2$,$\mathbf{q}_3$)-satellites appeared which were diffuse at the beginning but became sharp in two dimensions at *ca* 140–120 K (Kusz & Böhm, 1993). Although they still remained elongated in the direction of c*, the integral intensity of these diffuse reflections was collected at 100 ± 1 K; there was no substantial change of either shape or intensity of the reflections on further cooling. The data of this LT phase have been collected using the θ–2θ scan technique. The lattice parameters of the supercell were determined from 25 high-order reflections.

Main reflections 8,4,$\bar{1}\bar{2}$, $\bar{8}$,$\bar{4}$,12 and $\bar{8}$,4,$\bar{1}\bar{2}$ were used as standard reflections for monitoring intensity variations; in this case there was a maximum variation of 5%. For comparison, data have also been collected at room-temperature. In Table 1 the R-equivalent values are shown for the 100 K data after the merge in $P4/m$. Corrections were made for Lorentz and polarization effects and for absorption (μ = 224.1 cm^{-1}); $|F_{obs}| > 3\sigma$. In the refinement calculations, the standard parameter for isotropic secondary extinction was included; in different refinements, the value was *ca* 5 × 10^{-5}.

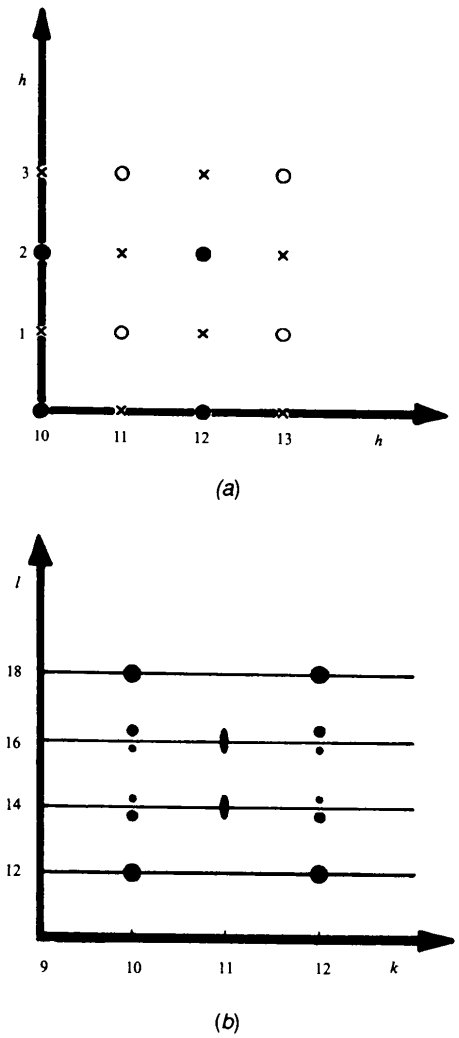

Fig. 2. Schematic diagram of the reflections investigated in the present studies: (*a*) The projection on the (a_1*,a_2*) plane; main reflections (solid circles), $\mathbf{q}_1$-satellites (open circles) and ($\mathbf{q}_2$,$\mathbf{q}_3$)-satellites (crosses). (*b*) The (a_2*,c*) plane; $\mathbf{q}_1$-satellites of second- and fourth-order are drawn separately, the ($\mathbf{q}_2$,$\mathbf{q}_3$)-satellites are elongated.

Table 1. *Parameters of the X-ray data collection*

	RT	100 K	
$2\theta_{max}$ (°)	36	80	
hkl_{max}	$-20 > hkl > 20$	$-40 > hkl > 40$	
Number of reflections			
total	3263	37347	
main reflections	1075	7066	
$\mathbf{q}_1$-satellites	2188	16791	
$(\mathbf{q}_2,\mathbf{q}_3)$-satellites	—	13490	
Merged in *P4/m*			R_{eq}
total	606*	4604	0.058
main reflections	268	941	0.055
$\mathbf{q}_1$-satellites	338	2150	0.062
$(\mathbf{q}_2,\mathbf{q}_3)$-satellites	—	1513	0.081
Unit cell	$2a_0 = 12.993$ (2)	$2a_0 = 12.967$ (2)	
	$3c_0 = 20.501$ (7)	$3c_0 = 20.465$ (5)	
Refinement programs	*SHELX*76 (Sheldrick, 1976)		
	MSRLSQ (Paciorek & Uszynski, 1987)		
	PROMETHEUS (Zucker *et al.*, 1983)		

* In *P4/mcc*, only 428 reflections were conforming with the extinction rules.

3. Structure determination

Average structure

The metric of the cell $a_0 \times b_0 \times c_0$ for the average structure requires that columns *A–D* in Fig. 1(*b*) are identical ($A = B = C = D$). Based on the main reflections alone, the basic structure was determined for the data set of 100 K in order to compare with the average structure at room temperature. The calculations were carried out with the program *SHELX*76 (Sheldrick, 1976). The final atomic coordinates are shown in Table 2. They agree very well with the corresponding parameters of the room-temperature phase (Böhm & von Schnering, 1985).*

Low-temperature (LT) structure

At 100 K the $\mathbf{q}_1$-satellites are incommensurate. The related structure is therefore incommensurate at the room-temperature phase. The metric [cell $(2)^{1/2}a_0 \times (2)^{1/2}a_0$] requires that columns $A = B$ and $C = D$ in Fig. 1(*b*). At first, the structure of the 100 K data set has been refined without the $(\mathbf{q}_2,\mathbf{q}_3)$-satellites. For comparison, the refinement was carried out in (3 + 1) dimensional space in the same superspace group $W^{P4/mcc}_{1\,111}$, used by van Smaalen, Bronsema & Mahy (1986) for the incommensurable room-temperature phase. For the calculations, the least-squares refinement program *MSRLSQ* (Paciorek & Uszynski, 1987) has been applied. The modulation function of the individual atom μ is described by the

* A list of structure factors has been deposited with the IUCr (Reference: SE0142). Copies may be obtained through The Managing Editor, International Union of Crystallography, 5 Abbey Square, Chester CH1 2HU, England.

Table 2. *Atomic coordinates for the average structure at* 100 K *and at room temperature (for comparison)*

For the cell, $(2)^{1/2}a_0 \times c_0$, *C*4/*mcc*, U_{ij} (Å^2)

Parameter		RT	100 K
Nb	x	0.0	0.0
	y	0.0	0.0
	z	0.25	0.25
	$U_{11} = U_{22}$	0.0036 (45)	0.0023 (6)
	U_{33}	0.0508 (90)	0.0618 (22)
Te	x	0.2362 (4)	0.2362 (1)
	y	0.0924 (4)	0.0921 (1)
	z	0.0	0.0
	U_{11}	0.0135 (35)	0.0136 (5)
	U_{22}	0.0075 (35)	0.0056 (5)
	U_{33}	0.0103 (38)	0.0067 (5)
	U_{12}	−0.0033 (16)	−0.0039 (3)
	No. ref	90	396
	R	0.050	0.045

Table 3. *Atomic parameters of the incommensurate structure at* 100 K [*without* $(\mathbf{q}_2,\mathbf{q}_3)$*-satellites*] *and (for comparison) at room temperature for the cell* $(2)^{1/2}a_0 \times c_0$, U_{ij} (Å^2); *superspace group* $W^{P4/mcc}_{1\,111}$,

		RT	100 K
Nb	x	0.0	0.0
	y	0.0	0.0
	z	0.25	0.25
	$u^s_{z,1}$	−0.0376 (3)	−0.0368 (3)
	$u^s_{z,2}$	0.0173 (3)	0.0188 (3)
	$U_{11} = U_{22}$	0.0045 (21)	0.0028 (4)
	U_{33}	0.0101 (33)	0.0054 (7)
Te	x	0.2361 (2)	0.2359 (1)
	$u^c_{x,1}$	0.0138 (1)	0.0139 (1)
	$u^s_{x,2}$	−0.0035 (1)	−0.0039 (1)
	y	0.0919 (1)	0.0921 (1)
	$u^c_{y,1}$	−0.0067 (1)	−0.0066 (1)
	$u^s_{y,2}$	−0.0010 (1)	−0.0010 (1)
	z	0.0	0.0
	$u^s_{z,1}$	−0.0066 (3)	−0.0065 (1)
	$u^s_{z,2}$	−0.0030 (3)	−0.0032 (1)
	U_{11}	0.0058 (18)	0.0040 (3)
	U_{22}	0.0061 (16)	0.0031 (16)
	U_{33}	0.0086 (18)	0.0047 (3)
	U_{12}	0.0002 (8)	−0.0002 (2)
	No. ref	428	1598
	R(all)	0.069	0.074
	R(main)	0.049	0.042
	$R(\mathbf{q}_1$-sat)	0.108	0.12

Fourier series expansion

$$u_i^{\mu}(t) = \sum_{n>0} \{u_{i,n}^{\mu,c} \cos[2\pi n(t_0^{\mu}+t)] + u_{i,n}^{\mu,s} \sin[2\pi n(t_0^{\mu}+t)]\},$$

where $u_{i,n}^{\mu,c}$ and $u_{i,n}^{\mu,s}$ are the amplitudes of the nth-order Fourier component of the atom μ; $t_0^{\mu} = \mathbf{q}\cdot\bar{x}_i^{\mu}$. In this case, the modulation function was limited to first- and second-order harmonics. Again the parameters agree very well with the corresponding values of the room-temperature phase (Table 3) and also with the values determined by van Smaalen, Bronsema & Mahy (1986). The smaller values of U_{ij} at 100 K are a temperature effect.

This means that the incommensurate structure based on the sharp satellite reflections remains the same also at 100 K. However, because of the ($\mathbf{q}_2$,$\mathbf{q}_3$)-satellites, an additional modulation occurs with a modulation period of $\sim 2/3c^*$. An electron diffraction experiment reveals that the ($\mathbf{q}_2$,$\mathbf{q}_3$)-satellites develop into some closely spaced satellites (Boswell & Prodan, 1986), which must be associated with long period commensurate domains of $16c_0$ and $32c_0$. The separation is beyond the resolution of conventional X-ray diffraction methods, therefore, the ($\mathbf{q}_2$,$\mathbf{q}_3$)-satellites will be taken as commensurate at the peak intensity $2/3c^*$.

If the structure based on the incommensurate $\mathbf{q}_1$-satellites is approximated by a threefold superstructure in direction c, the same solution is obtained as for the room-temperature phase by Böhm & von Schnering (1985), *i.e.* two columns (*A* and *C* in Fig. 1) formed by Nb_3 groups. However, this solution is not unique. A second solution of equal quality is obtained, with Nb_3 groups in one chain and Nb_2 groups and isolated Nb atoms in the second chain, if the starting conditions for the refinement are changed. This solution determined with the program *PROMETHEUS* (Zucker, Perenthaler, Kuhs, Bachmann & Schulz, 1983) is shown in Fig. 3. The *R*-value is very similar ($R = 0.064$) to the alternative solution; obviously there are two minima in the refinement of the residuum. Since both models are approximations of the exact solution, each model apparently reflects different aspects of the exact structure. One may suspect that in the real incommensurate structure, the features of both solutions are present, *i.e.* a sequence of Nb_3 (approximately 75%) and Nb_2 groups and isolated Nb atoms (approximately 25%). This sequence should have a period of $16c_0$ of the basic structure (*i.e.* $\mu = 3.2$). This would imply that the incommensurate structure is a string of eight Nb-triplets bordered by a group of Nb_2–Nb–Nb_2–Nb–Nb_2. As $\mathbf{q}_1$-satellites of odd order are observed around the position of extinct main reflections and those of even order are found around observed main reflections, the modulation function of Nb in 00z should have a phase shift of π with respect to that in $\frac{11}{22}z$. The same two super structure approximations of the incommensurate structure can be verified for both the room-temperature data and the 100 K data.

If all reflections [also the ($\mathbf{q}_2$,$\mathbf{q}_3$)-satellites] are taken into account, the metric of the structure corresponds to the cell $2a_0 \times 2a_0$ [Fig. 1(*b*)]. At least three of the four columns *A*, *B*, *C* and *D* must be different; the fourfold symmetry requires that $C = D$. In order to determine the low-temperature structure, one may ask in what respect does this phase deviate from the incommensurate phase at 100 K (Table 3), which was determined without the ($\mathbf{q}_2$,$\mathbf{q}_3$)-satellites. The answer is given by a structure which is calculated by the ($\mathbf{q}_2$,$\mathbf{q}_3$)-satellites alone.

This structure ('complement structure') is a difference structure with positive and negative density exhibiting the deviations from the incommensurate phase. It can be calculated by a Fourier synthesis which is based on the phases of the incommensurate structure as approximated by a threefold superstructure and on the intensities of the ($\mathbf{q}_2$,$\mathbf{q}_3$)-satellites. For the phases, two superstructure approximations could be used as mentioned above: one model with two Nb_3 chains and another model with Nb_3 and Nb_2 chains (Fig. 3). Fig. 4 shows the Fourier map of the complement structure; the sections $y = 0$ and $y = 0.5$ in the (a,c) plane are exhibited. These sections show the chains of Nb atoms along c and the columns *A*–*C* and *D*–*B* of Fig. 1(*b*), respectively. In Fig. 4(*a*), there is no density at the positions of the Nb atoms in column *C* (crosses in Fig. 4); the same is true for column *D* in Fig. 4(*b*). This means that columns *C* and *D*, which are identical in the incommensurate phase, remain unchanged.

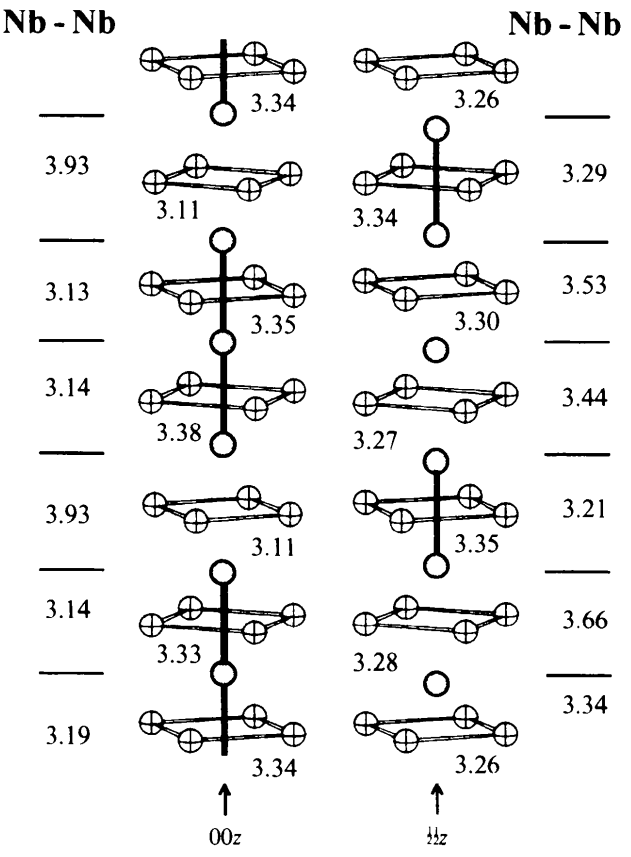

Fig. 3. Alternative solution: the superstructure approximation of the average structure (main and $\mathbf{q}_1$-satellite) of the low-temperature phase of $NbTe_4$ with interatomic distances Nb—Nb and Te—Te.

Columns *A* and *B* show positive and negative densities about the positions of Nb (crosses in Fig. 4). They refer to the shifts of Nb atoms from the positions of the incommensurate phase, which is here described as a threefold superstructure approximation in the *c* direction. These shifts are anti-phase in *A* and *B*; when the density is positive in the complement structure of *A*, it is negative in that of *B*. Therefore, the commensurate approximation of the low-temperature phase is characterized by a structure in which *A* and *B* are different, while *C* and *D* are identical. In the same way, the sections $z = \text{const.}$ (a_1,a_2) plane can be analysed showing the correlated Te shifts. The Te squares perform clockwise–anticlockwise rotations which are coupled either between columns *A* and *B* or between *C* and *D*. If there is a strong rotation in *A* and *B* in the complement structure, there is little rotation in *C* and *D* and *vice versa*. These rotations alternate between *A*–*B* and *C*–*D* for the six Te squares along *c*. The result of Fig. 4 is the same, no matter from which model the phases are taken. It is interesting to note that Prodan *et al.* (1990) earlier proposed these atomic shifts for the low-temperature phase on the basis of model calculations in order to reproduce the electron diffraction pattern with sharp $(\mathbf{q}_2,\mathbf{q}_3)$-satellites ($LT_1$ and LT_2). These authors conjectured that their LT_1/LT_2 model is a precursor phase of the commensurate low-temperature (C) phase. In fact, their model differs from the present superstructure approximation for the low-temperature phase by the postulated existence of discommensurations in the low-temperature phase in order to account for the incommensurate (long period commensurate) superstructure of $\sim 32c_0$. The sequence of Nb_3 groups between the discommensurations is the same as in the present commensurate model for the low-temperature phase which is derived from the X-ray data.

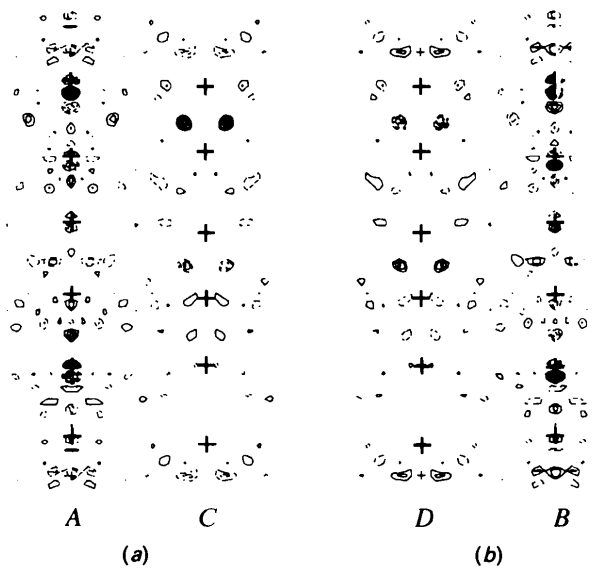

Fig. 4. Fourier synthesis of the threefold superstructure (complement structure) at 100 K, (*a*,*c*) plane; (*a*) $y = 0$ and (*b*) $y = 0.5$.

Based on the model derived from the complement structure, the structure has been refined in the space group *P*4, with all 4604 reflections (main and satellite reflections) as a $(2 \times 2 \times 3)$-fold super structure; the *R*-value converged to $R = 0.060$; the parameters are shown in Table 4. In the space group *P*4, there are twofold axes in columns *C* and *D* and fourfold axes in *A* and *B*. Therefore, the Te atoms in *A* and *B* must form squares by symmetry, the Te atoms in *C* and *D* may form rectangles; in fact, slight distortions occur; the interatomic distances for the columns *A*, *B*, *C* = *D* are shown in Fig. 5. The anisotropic temperature coefficients were taken to be the same by constraints within each species of atoms.

4. Discussion

The incommensurate low-temperature structure with diffuse $(\mathbf{q}_2,\mathbf{q}_3)$-satellites at commensurate positions was determined as a threefold superstructure approximation in the *c* direction by evaluating the complement structure, which describes the deviation of density from the incommensurate phase. In the superstructure approximation without $(\mathbf{q}_2,\mathbf{q}_3)$-satellites, columns *C* and *D* are the same; they are formed by chains of Nb_3 groups. Columns *A* and *B* are also identical. The complement structure implies that the Nb atoms in columns *A* and *B* are shifted, whereas the Nb atoms in *C* and *D* remain unchanged. The shifts occur in such a way that there is a phase shift of $2\pi/3$ between adjacent columns. If a reference point of *A* is on, say, $z = 0$, it is on $z = 1/3$ in *C*, on $z = 2/3$ in *B* and again on $z = 1/3$ in *D*. The Nb shifts in *A* and *B* are in fact small in order to change a bonding to a non-bonding distance and *vice versa* (see Fig. 6). Two starting configurations can be visualized: one configuration with chains of Nb_3 groups in $C = D$ and Nb_2–Nb groups in $A = B$ [Fig. 6(*a*)]; another configuration with chains of Nb_3 groups alone [Fig. 6(*b*)]. Both configurations yielded the same result of columns of Nb_3 groups with a phase shift of $2\pi/3$ with respect to each other.

It must be emphasized, however, that the structure described above has long-range order only in two dimensions. It is a short-range model for the structure along *c*; since the $(\mathbf{q}_2,\mathbf{q}_3)$-satellites still remain elongated along c^*. In the real structure, the incommensurateness still remains. We must assume that discommensurations (*e.g.* Nb_2 groups) cause the incommensurateness, as was observed by Mahy, van

Table 4. *Atomic parameters of the LT phase (commensurate approximation) of* $NbTe_4$ *in the cell* $2a_0 \times 2b_0 \times 3c_0$, *space group* = $P4$, U_{ij} ($Å^2$) *unique reflections*; *No. ref* = 4604; $R = 0.060$ ($R_{main} = 0.047$, $R_{q_1} = 0.063$, $R_{q_{2,3}} = 0.131$)

	x	y	z		x	y	z
Nb*A*1	0.0	0.0	0.0915 (5)	Te*A*1	0.0631 (3)	0.1560 (3)	0.0000 (2)
Nb*A*2	0.0	0.0	0.2409 (5)	Te*A*2	0.1693 (3)	0.0734 (3)	0.1691 (2)
Nb*A*3	0.0	0.0	0.3978 (5)	Te*A*3	0.0802 (3)	0.1635 (3)	0.3290 (2)
Nb*A*4	0.0	0.0	0.5925 (5)	Te*A*4	0.1557 (3)	0.0626 (3)	0.4996 (2)
Nb*A*5	0.0	0.0	0.7513 (5)	Te*A*5	0.0749 (3)	0.1691 (3)	0.6683 (2)
Nb*A*6	0.0	0.0	0.9022 (5)	Te*A*6	0.1633 (3)	0.0760 (3)	0.8294 (2)
Nb*B*1	0.5	0.5	0.0693 (5)	Te*B*1	0.5684 (3)	0.6670 (3)	−0.0033 (3)
Nb*B*2	0.5	0.5	0.2458 (5)	Te*B*2	0.6615 (3)	0.5705 (3)	0.1643 (3)
Nb*B*3	0.5	0.5	0.4091 (5)	Te*B*3	0.5791 (3)	0.6670 (4)	0.3319 (3)
Nb*B*4	0.5	0.5	0.5700 (6)	Te*B*4	0.6663 (3)	0.5683 (3)	0.4974 (3)
Nb*B*5	0.5	0.5	0.7561 (5)	Te*B*5	0.5716 (3)	0.6619 (3)	0.6647 (3)
Nb*B*6	0.5	0.5	0.9110 (6)	Te*B*6	0.6666 (3)	0.5818 (3)	0.8321 (3)
NbC1	0.5	0.0	0.0758 (3)	TeC11	0.5798 (3)	0.1668 (4)	−0.0005 (2)
NbC2	0.5	0.0	0.2364 (2)	TeC12	0.3349 (4)	0.0751 (4)	−0.0002 (2)
NbC3	0.5	0.0	0.4288 (3)	TeC21	0.6668 (3)	0.0754 (3)	0.1622 (2)
NbC4	0.5	0.0	0.5844 (4)	TeC22	0.4271 (3)	0.1668 (4)	0.1629 (2)
NbC5	0.5	0.0	0.7339 (3)	TeC31	0.5621 (3)	0.1605 (3)	0.3316 (2)
NbC6	0.5	0.0	0.9241 (3)	TeC32	0.3414 (3)	0.0629 (3)	0.3305 (2)
				TeC41	0.6665 (4)	0.0765 (4)	0.5
Nb	$U_{11} = U_{22} = 0.0021$ (1)			TeC42	0.4203 (3)	0.1653 (4)	0.4999 (2)
	$U_{33} = 0.0052$ (1)			TeC51	0.5730 (3)	0.1682 (3)	0.6626 (2)
Te*A*1	$U_{11} = 0.0059$ (1)			TeC52	0.3346 (3)	0.0747 (3)	0.6621 (3)
	$U_{22} = 0.0024$ (1)						
	$U_{33} = 0.0048$ (1)			TeC61	0.6589 (3)	0.0610 (3)	0.8300 (2)
	$U_{12} = 0.0016$ (1)						
	$U_{13} = 0.0000$ (2)			TeC62	0.4358 (3)	0.1603 (4)	0.8317 (2)
	$U_{23} = -0.0000$ (2)						

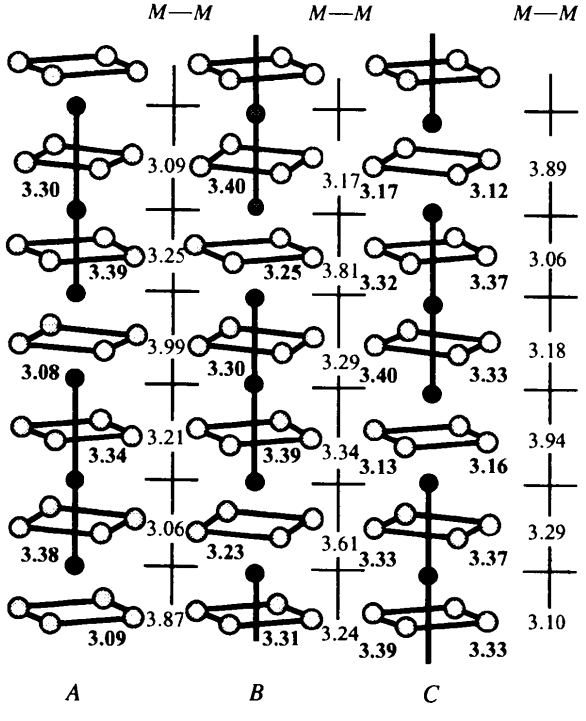

Fig. 5. The columns *A*, *B*, *C* = *D* with interatomic distances (Å) within the plane Te groups and between the Nb atoms for the low-temperature phase (Table 4).

Landuyt, Amelinckx, Bronsema & van Smaalen (1986) and postulated by Prodan *et al.* (1990) in their model calculations. These discommensurations remain metastable as defects and they pin the incommensurate low-temperature structure even at temperatures below 50 K (Kusz & Böhm, 1993).

The $TaTe_4$ and $NbTe_4$ average structures are isostructural and the idea that room-temperature $TaTe_4$ has the same modulation as the low-temperature lock-in phase of $NbTe_4$ has been put forward several times. The room-temperature structure of $TaTe_4$ is modulated with $q1$, $q2$ and $q3$ already at room temperature with commensurate components equal to $2/3c^*$ for all three wavevectors. The structure was determined by Bronsema *et al.* (1987) in the $2a_0 \times 2b_0 \times 3c_0$ supercell with space group $P4/ncc$. Budkowski *et al.* (1989) confirmed the result using the superspace formalism. It is interesting to compare the $(2 \times 2 \times 3)$-fold superstructure of $TaTe_4$ with the $(2 \times 2 \times 3)$-fold superstructure approximation of low-temperature $NbTe_4$. In this paper, the low-temperature structure was refined in the space group $P4$ because 190 out of 4605 reflections ($|F_{obs}| > 3\sigma$) violate the rules for absences in $P4/ncc$ or $P4cc$. A $\lambda/2$ effect can be excluded since the violation is also observed at 30 kV for Mo $K\alpha$. In the solution of $P4$ also, the deviations from a *c*-glide are greater than the error bars. Since the $\mathbf{q}_1$-satellites are in fact (not in our approximation) incommensurate, the atoms along *c* must not be related by constraints of a glide plane or any other symmetry element. It is interesting to note that the same structure with a phase shift of $2\pi/3$ between adjacent columns was determined for our commensurate

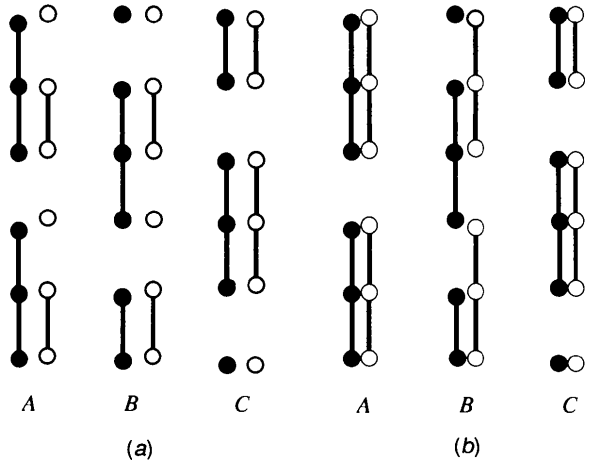

Fig. 6. The chains of Nb in the commensurate low-temperature phase (solid circles) for the three columns *A*, *B* and *C*; the open circles indicate the starting configuration at the beginning of the refinement; (*a*) starting configuration was chains of Nb_3 and Nb_2–Nb groups; (*b*) starting configuration was only Nb_3 groups.

approximation of the low-temperature phase of $NbTe_4$ and for the commensurate room-temperature structure of $TaTe_4$.

The project has been supported by a grant of the Deutsche Forchungsgemeinschaft, local support was given by the Materialwissenschaftliches Forschungszentrum der Universität Mainz. The authors thank J. C. Bennet (Waterloo, Ontario) who supplied the single crystals for comparative measurements.

References

BÖHM, H. & VON SCHNERING, H.-G. (1983). *Z. Kristallogr.* **162**, 26–27.
BÖHM, H. & VON SCHNERING, H.-G. (1985). *Z. Kristallogr.* **171**, 41–64.
BOSWELL, F. W. & PRODAN, A. (1986). *Phys. Rev. B*, **34**, 2979–2981.
BOSWELL, F. W., PRODAN, A. & BRANDON, J. K. (1983). *J. Phys. C*, **16**, 1067–1076.
BRONSEMA, K. D., VAN SMAALEN, S., DE BOER, J. L., WIGERS, G. A., JELLINEK, F. & MAHY, J. (1987). *Acta Cryst.* **B43**, 305–313.
BUDKOWSKI, A., PRODAN, A., MARINKOVIC, V., KUCHARCZYK, D., USZYNSKI, I. & BOSWELL, F. W. (1989). *Acta Cryst.* **B45**, 529–534.
EAGLESHAM, D. J., BIRD, D., WITHERS, R. L. & STEEDS, J. W. (1985). *J. Phys. C*, **18**, 1–11.
KUSZ, J. & BÖHM, H. (1992). *Z. Kristallogr.* **201**, 9–17.
KUSZ, J. & BÖHM, H. (1993). *Z. Kristallogr.* **208**, 187–194.
MAHY, J., VAN LANDUYT, J., AMELINCKX, S., BRONSEMA, K. D. & VAN SMAALEN, S.(1986). *J. Phys. C*, **19**, 5049–5069.
PACIOREK, W. A. & USZYNSKI, I. (1987). *J. Appl. Cryst.* **20**, 57–59.
PRODAN, A., BOSWELL, F. W., BENNET, J. C., CORBETT, J. M., VIDMAR, T., MARINKOWIC, V. & BUDKOWSKI, A. (1990). *Acta Cryst.* **B46**, 587–591.
SELTE, K. & KJEKSHUS, A. (1964). *Acta Chem. Scand.* **18**, 690–696.
SHELDRICK, G. M. (1976). *SHELX76. Program for Crystal Structure Determination*. Univ. of Cambridge, England.
SMAALEN, S. VAN, BRONSEMA, K. D. & MAHY, J. (1986). *Acta Cryst.* **B42**, 43–50.
ZUCKER, U. H., PERENTHALER, E., KUHS, W., BACHMANN, R. & SCHULZ, H. (1983). *J. Appl. Cryst.* **16**, 358–362.

Acta Cryst. (1994). **B50**, 655–662

Structure and Non-Linear Optical Properties of $KTiOAsO_4$

BY S. C. MAYO*

Clarendon Laboratory, Parks Road, Oxford OX1 3PU, England

P. A. THOMAS† AND S. J. TEAT

Department of Physics, University of Warwick, Coventry CV4 7AL, England

AND G. M. LOIACONO AND D. N. LOIACONO

Crystal Associates Inc., Waldwick, NJ 07463, USA

(*Received* 16 *February* 1994; *accepted* 2 *June* 1994)

Abstract

Refinements of the crystal structures of potassium titanyl arsenate, $KTiOAsO_4$, grown from a tungstate flux (1) and an arsenate flux (2), are reported. Crystal data at room temperature are: (1) $KTiOAsO_4$, orthorhombic, $Pna2_1$, $a = 13.138$ (2), $b = 6.582$ (1), $c = 10.787$ (2) Å, $Z = 8$, $R = 0.027$ for 2086 reflections with $I > 3\sigma(I)$; (2) $KTiOAsO_4$, orthorhombic, $Pna2_1$, $a = 13.130$ (2), $b = 6.581$ (1), $c = 10.781$ (1) Å, $Z = 8$, $R = 0.020$ for 2716 observed reflections with $I > 3\sigma(I)$. The values of the linear and non-linear optical susceptibilities for $KTiOAsO_4$ are discussed using the isostructural non-linear optical crystal $KTiOPO_4$ as a starting point. The observed increase in certain non-linear optical coefficients of $KTiOAsO_4$ is shown to derive principally from the increase in the linear refractive indices brought about by the substitution of phosphorus by arsenic in the structure.

Introduction

Potassium titanyl phosphate, $KTiOPO_4$ (KTP), and its analogues have been of interest for many years because of their suitability for non-linear optical applications (Zumsteg, Bierlein & Gier, 1976). In particular, KTP is known as a highly efficient frequency doubler for 1.06 μm radiation (Perkins & Fahlen, 1987). The isostructural analogue

* Present address: Research School of Chemistry, Australian National University, Canberra, ACT0200, Australia.
† Author for further correspondence.